

# Control of mutual spatial coherence of temporal features by reflexive photorefractive coupling

A. A. Zozulya and D. Z. Anderson

*Joint Institute for Laboratory Astrophysics, University of Colorado and National Institute of Standards and Technology, Campus Box 440, Boulder, Colorado 80309-0440*

M. Saffman

*Department of Optics and Fluid Dynamics, Risø National Laboratory, Postbox 49, DK-4000 Roskilde, Denmark*

Received May 24, 1995; revised manuscript received August 24, 1995

We analyze reflexive photorefractive coupling of an information-bearing beam carrying several distinct spatiotemporal features, with emphasis on the coupling-induced change in the mutual spatial coherence. We formulate equations describing evolution of the mutual correlation functions between different features and discuss their solutions both in the full two-dimensional case and in the limit leading to a one-dimensional description of the reflexive coupling geometry. © 1996 Optical Society of America

## 1. INTRODUCTION

Recent papers have shown that reflexive photorefractive coupling, in which a light beam consisting of several spatiotemporal features interacts with a copy of itself in a photorefractive medium, can be used to modify the information content of the light coherence of spatially identical beams,<sup>1,3</sup> to ensure single-frequency oscillation in photorefractive ring-resonator circuits,<sup>5,6</sup> and also (allowing for a path-length difference between the two beams in Fig. 1) to obtain frequency narrowing of a laser line.<sup>7</sup>

Previous analysis of reflexive coupling was based mostly on one-dimensional models. A recent paper<sup>4</sup> analyzed manipulation of the intensity of selected features and modification of their spatial overlap. Changes in the coherence properties of the interacting features have been analyzed in the framework of a one-dimensional model<sup>1</sup> and, in the limit of spatially constant pumping beams, of a two-dimensional model.<sup>2,3</sup> The present paper is aimed at discussing aspects of the reflexive coupling geometry pertinent to a change of the spatial coherence properties of the interacting temporal features in the framework of a two-dimensional model and at establishing the transition to the one-dimensional limit.

Consider an information-bearing laser beam with carrier frequency  $\omega$  and wave number  $k$  consisting of  $N$  spatiotemporal features (signals):

$$E(\mathbf{r}, t) = \sum_{j=1}^N c_j(t) e_j(\mathbf{r}) \exp[i(kz - \omega t)]. \quad (1)$$

This beam is divided by a beam splitter into two beams:

$$E^{\pm} = \sum_{j=1}^N c_j(t) e_j^{\pm}(\mathbf{r}), \quad (2)$$

which interact in a photorefractive medium (see Fig. 1). We refer below to beams  $E^+$  and  $E^-$  as gain and loss beams, respectively, in accordance with the direction of energy transfer in Fig. 1. Each feature in the initial

beam [Eq. (1)] is the image  $e_j(\mathbf{r})$  with the time dependence  $c_j(t)$ . We assume that the average intensity of each feature does not depend on time and that the features are temporally orthogonal in the photorefractive medium. Temporal orthogonality means that the product of any two different temporal amplitudes averaged over times comparable with or larger than the characteristic relaxation time  $\tau$  of the photorefractive medium is equal to zero:  $\int_{-\infty}^t dt' c_i(t') c_j^*(t') \exp[(t' - t)/\tau] = \delta_{i,j}$ . Temporal orthogonality of the features implies that the photorefractive medium does not respond to the interference pattern that is due to any pair of different temporal components of beams  $E^+$  and  $E^-$  and that these components do not interact directly with each other. The steady-state grating written in the photorefractive medium by the beams (2) is formed only by features with the same temporal dependencies:

$$G(\mathbf{r}) = \frac{\Gamma}{2I_T} \sum_{j=1}^N e_j^+(\mathbf{r}) e_j^{-*}(\mathbf{r}), \quad (3)$$

where  $\Gamma$  is the nonlinear coupling coefficient and  $I_T(\mathbf{r}) = \sum_{j=1}^N (|e_j^+(\mathbf{r})|^2 + |e_j^-(\mathbf{r})|^2)$  is the total local intensity in the medium.

Despite the fact that each temporal signal interacts directly only with itself, the total grating [Eq. (3)] couples all of them. One reason is that the amount of nonlinear coupling experienced by each signal is affected by the intensities of all the other signals because of the presence of the total intensity in the denominator of expression (3). The second reason is that a signal may scatter off the grating written by another pair of signals if those signals are (partially) spatially correlated. This indirect coupling results in changes in both the intensities and the spatial coherence properties of the temporal features at the output, as is shown below.

The structure of the paper is as follows: Section 2 we start with dynamical equations for multifrequency two-

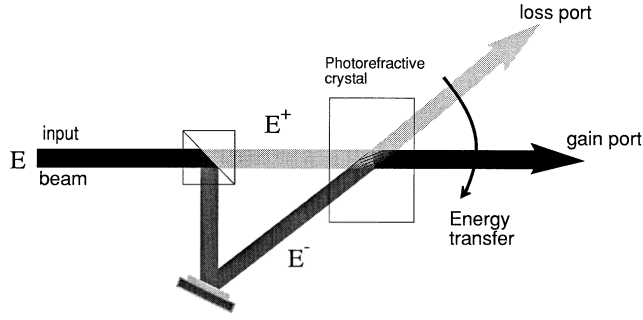


Fig. 1. Photorefractive reflexive coupling geometry.

beam coupling in a photorefractive medium. We then review briefly the formalism of transverse correlation functions used to describe statistical properties of information-carrying (speckled) beams and formulate equations governing the evolution of partially spatially correlated temporal features in terms of mutual correlation functions. In Section 3 we discuss parameters that determine the geometry of interaction in the case of full or partial overlap of the interacting beams inside the nonlinear medium. We show that general equations for partially spatially correlated temporal features can, under certain assumptions, be cast in a diagonalized form, corresponding to a set of spatially uncorrelated fields, by means of a unitary transformation. Section 4 is devoted to the analysis of asymptotic properties of solutions of the previously formulated equations, and numerical results are given in Section 5. Section 6 is a summary.

## 2. GENERAL EQUATIONS

Paraxial evolution of the slowly varying amplitudes  $e_i^\pm$  [Eq. (2)] in the photorefractive medium is governed by the equations

$$\left( \frac{\partial}{\partial l_+} - \frac{i}{2k} \Delta_{\perp,+} \right) e_i^+ = \frac{\Gamma}{2I_T} \left( \sum_{j=1}^N e_j^+ e_j^{-*} \right) e_i^-, \quad (4a)$$

$$\left( \frac{\partial}{\partial l_-} - \frac{i}{2k} \Delta_{\perp,-} \right) e_i^- = -\frac{\Gamma}{2I_T} \left( \sum_{j=1}^N e_j^{+*} e_j^- \right) e_i^+, \quad (4b)$$

where  $l_\pm$  are directions of propagation of beams  $E_\pm$ ,  $\Delta_{\perp,\pm}$  are Laplace operators acting on coordinates perpendicular to these directions, and the coupling constant  $\Gamma$  has been assumed real.

Solution of Eqs. (4) requires specification of all input field distributions. In the case of image-bearing (speckled) beams these distributions are often unknown, and the beams may be characterized only in terms of their statistical properties. The standard procedure in this case is to derive from Eqs. (4) a set of statistically averaged equations for transverse correlation functions of the beams. Below we recall this procedure, using a textbook example<sup>8</sup> of the free propagation of an image-bearing (speckled) beam  $e(\mathbf{r}_\perp, z)$ , governed by the equation

$$\left( \frac{\partial}{\partial z} - \frac{i}{2k} \Delta_{r_\perp} \right) e(\mathbf{r}_\perp, z) = 0. \quad (5)$$

The transverse two-point correlation function  $\mathcal{E}(\mathbf{r}_{\perp,1}, \mathbf{r}_{\perp,2}, z) \equiv \langle e^*(\mathbf{r}_{\perp,1}, z) e(\mathbf{r}_{\perp,2}, z) \rangle$ , where  $\langle \dots \rangle$  means

a statistical (ensemble) average, obeys the equation following directly from Eq. (5):

$$\left[ \frac{\partial}{\partial z} - \frac{i}{2k} (\Delta_{r_{\perp,2}} - \Delta_{r_{\perp,1}}) \right] \mathcal{E}(\mathbf{r}_{\perp,1}, \mathbf{r}_{\perp,2}, z) = 0. \quad (6)$$

Introduction of new coordinates  $\boldsymbol{\rho} = \mathbf{r}_{\perp,2} - \mathbf{r}_{\perp,1}$ ,  $\mathbf{R} = (\mathbf{r}_{\perp,1} + \mathbf{r}_{\perp,2})/2$  casts Eq. (6) into the form

$$\left( \frac{\partial}{\partial z} - \frac{i}{k} \frac{\partial^2}{\partial \boldsymbol{\rho} \partial \mathbf{R}} \right) \mathcal{E}(\boldsymbol{\rho}, \mathbf{R}, z) = 0. \quad (7)$$

Consider the boundary condition for Eq. (7) of the form

$$\begin{aligned} \mathcal{E}(\mathbf{r}_{\perp,1}, \mathbf{r}_{\perp,2}, 0) \\ = \exp \left[ -\frac{r_{\perp,1}^2 + r_{\perp,2}^2}{2d^2} - \frac{(\mathbf{r}_{\perp,1} - \mathbf{r}_{\perp,2})^2}{\rho_c^2} + ik \frac{r_{\perp,1}^2 - r_{\perp,2}^2}{2f} \right] \end{aligned}$$

or, equivalently,

$$\begin{aligned} \mathcal{E}(\boldsymbol{\rho}, \mathbf{R}, 0) = \exp \left( -\frac{R^2}{2d^2} - \frac{\rho^2}{\rho_{\text{eff}}^2} - ik \frac{\boldsymbol{\rho} \mathbf{R}}{f} \right), \\ \rho_{\text{eff}}^{-2} = \rho_c^{-2} + (1/4)d^{-2}, \quad (8) \end{aligned}$$

representing a beam that at  $z = 0$  is characterized by the total diameter  $d$ , the transverse correlation radius  $\rho_c$ , and a finite radius of curvature owing to its passage through a lens of focal length  $f$ .

Solution of Eq. (7) with boundary condition (8) yields

$$\begin{aligned} \mathcal{E}(\boldsymbol{\rho}, \mathbf{R}, z) = g(z) \exp \left[ -g(z) \left( \frac{R^2}{2d^2} + \frac{\rho^2}{\rho_{\text{eff}}^2} \right) \right. \\ \left. - i \frac{k}{2} \boldsymbol{\rho} \mathbf{R} \frac{d}{dz} \ln g(z) \right], \quad (9) \end{aligned}$$

where  $g(z)^{-1} = [1 - 2zf^{-1} + z^2(f^{-2} + l_d^{-2})]$ ,  $l_d = k\rho_{\text{eff}}d/2$ .

According to Eq. (9) the evolution along the coordinate  $z$  of the diameter and the characteristic correlation radius of the beam are determined by the value of the diffraction length  $l_d$ . If we take  $d = 0.5$  mm,  $\rho_c = 10$   $\mu\text{m}$ , and  $\lambda = 0.5$   $\mu\text{m}$ , then  $l_d \approx 30$  mm. In typical photorefractive experiments the nonlinear medium interaction length  $l_{\text{int}}$  is approximately 2–5 mm, i.e.,  $l_{\text{int}} \ll l_d$ . Assuming also that  $l_{\text{int}} \ll f$ , this circumstance allows us to neglect diffraction effects in averaged equations for quadratic combinations of the fields  $e_i^+$  and  $e_i^-$ . Nonlinear interaction between the beams [Eqs. (4)] along with diffraction also changes both  $\rho_c$  and  $d$ . For reasonable values of the nonlinearity this can change the value of  $l_d$  two or three times (not orders of magnitude), so we may assume that if  $l_{\text{int}} \ll l_d$  at the input to the nonlinear medium this inequality holds throughout it. Physically under these conditions the beam as a whole looks well defined and collimated inside the interaction region, though the characteristic diffraction length of a single speckle may be short compared with the size of the nonlinear medium.

In what follows, we work with average intensities and mutual correlation functions  $\mathcal{E}_{i,j}^+(\mathbf{r}) = \langle e_i^{+*}(\mathbf{r}) e_j^+(\mathbf{r}) \rangle$  and

$\mathcal{E}_{i,j}^-(\mathbf{r}) = \langle e_i^{-*}(\mathbf{r})e_j^-(\mathbf{r}) \rangle$ . Equations for these functions follow directly from Eqs. (4) and have the form

$$\frac{\partial}{\partial l_+} \mathcal{E}_{i,j}^+(\mathbf{r}) = \frac{\Gamma}{2I_T} \sum_{l=1}^N (\mathcal{E}_{i,l}^+ \mathcal{E}_{l,j}^- + \mathcal{E}_{i,l}^- \mathcal{E}_{l,j}^+), \quad (10a)$$

$$\frac{\partial}{\partial l_-} \mathcal{E}_{i,j}^-(\mathbf{r}) = -\frac{\Gamma}{2I_T} \sum_{l=1}^N (\mathcal{E}_{i,l}^- \mathcal{E}_{l,j}^+ + \mathcal{E}_{i,l}^+ \mathcal{E}_{l,j}^-), \quad (10b)$$

$$I_T = \sum_{l=1}^N (\mathcal{E}_{i,l}^+ + \mathcal{E}_{i,l}^-). \quad (10c)$$

In deriving Eqs. (10) for the mutual correlation functions we used the approximation  $\langle e_i^{+*} e_j^+ e_l^{-*} e_k^- \rangle \approx \langle e_i^{+*} e_j^+ \rangle \langle e_l^{-*} e_k^- \rangle$ , neglecting higher-order terms proportional to the ratio  $\rho_c/d \ll 1$ . We also neglected the transverse Laplacians based on our analysis of Eqs. (5)–(9) and assuming that  $l_{\text{int}} \ll l_d, l_{\text{int}} \ll f$ . Note that the neglect of the diffraction effects in Eq. (10) is possible because the ensemble averaging removes fine speckle structure, leaving only large transverse scales of the order of the diameter of the beam. If we work with the first of Eqs. (4), all diffraction effects should be retained.

To formulate a boundary-value problem completely we should supplement Eqs. (10) by the boundary conditions specifying input values  $\mathcal{E}_{i,j}^{\pm}(\mathbf{r})_{\text{in}}$  for all  $1 \leq i, j \leq N$ . The diagonal terms here ( $i = j$ ) give averaged intensity distributions of the input beams, whereas nondiagonal terms determine the degree of spatial correlation between different temporal components, with nonzero values meaning that the corresponding components are partially correlated.

Along with correlation functions  $\mathcal{E}_{i,j}^{\pm}$  we use the normalized correlation functions  $h_{i,j}$ , defined as

$$h_{i,j}^{\pm} = \frac{\mathcal{E}_{i,j}^{\pm}(\mathbf{r})}{[\mathcal{E}_{i,i}^{\pm}(\mathbf{r})\mathcal{E}_{j,j}^{\pm}(\mathbf{r})]^{1/2}}. \quad (11)$$

Integral properties of the beams will be characterized by their input and output powers and integrated correlation functions  $P_{i,j}^{\pm, \text{in(out)}}$ , before (in) and after (out) the interaction region, and also by the normalized integrated correlation functions (overlaps)  $H_{i,j}^{\pm, \text{in(out)}}$  determined by the relations

$$P_{i,j}^{\pm, \text{in(out)}} = \int d\mathbf{r}_{\pm} \mathcal{E}_{i,j}^{\pm, \text{in(out)}}, \quad (12a)$$

$$H_{i,j}^{\pm, \text{in(out)}} = \frac{P_{i,j}^{\pm, \text{in(out)}}}{[P_{i,i}^{\pm, \text{in(out)}}P_{j,j}^{\pm, \text{in(out)}}]^{1/2}}. \quad (12b)$$

Note in conclusion that Eqs. (10) have the set of conservation integrals

$$P_{i,j}^{+, \text{in}} + P_{i,j}^{-, \text{in}} = P_{i,j}^{+, \text{out}} + P_{i,j}^{-, \text{out}}, \quad 1 \leq i, j \leq N. \quad (13)$$

### 3. INTERACTION GEOMETRY AND DIAGONALIZATION OF EQUATIONS

Solutions of Eqs. (10) depend on the value of the coupling constant  $\Gamma$ , the nonlinear medium length  $L$ , the characteristic diameters of the beams  $d$ , and the angle

$\theta$  between them or, more precisely, on some combination of these parameters. Indeed, Eqs. (10) can always be transformed into a new system of coordinates in which beams  $e_i^+$  and  $e_i^-$  propagate along two perpendicular axes.<sup>9</sup> If the angle between the beams equal  $\theta$  so that  $\partial/\partial l_{\pm} = \cos(\theta/2)(\partial/\partial x) \pm \sin(\theta/2)(\partial/\partial y)$ , then transition to the new system of coordinates  $(x', y')$

$$\begin{aligned} x' &= x \sin(\theta/2) + y \cos(\theta/2), \\ y' &= x \sin(\theta/2) - y \cos(\theta/2), \end{aligned} \quad (14)$$

results in the transformations  $\partial/\partial l_+ \rightarrow \partial/\partial x'$ ,  $\partial/\partial l_- \rightarrow \partial/\partial y'$ , and  $\Gamma \rightarrow \Gamma/\sin \theta$ . Transverse dimensions of the beams remain the same; the boundaries of the nonlinear medium  $x = \pm L/2$  are transformed into  $x' + y' = \pm L \sin(\theta)$ . All geometrical effects are determined uniquely by the parameter  $\delta = L \sin(\theta)/d$ , which is the relative displacement of beams  $e_i^+$  and  $e_i^-$  across the length of the nonlinear medium. If  $\delta \gg 1$  the rhombus-shaped beam overlap region lies completely inside the nonlinear medium, corresponding to a fully two-dimensional situation. The opposite case,  $\delta \ll 1$ , when the rhombus is mostly outside, may be characterized as the one-dimensional limit. In the one-dimensional case the nonlinearity is characterized by the product  $\Gamma L/\cos(\theta/2)$ . In the full two-dimensional case it may be taken as  $3\Gamma d/\sin(\theta)$ , this combination being the distance between the 10% intensity points of a Gaussian beam with diameter  $d$  crossing at the angle  $\theta$  (the choice of 10% points and the ensuing multiplicand 3 are somewhat arbitrary).

Because of their relatively complex structure Eqs. (10) do not permit immediate insight into the evolution of degrees of mutual correlation among different temporal features with the exception of the case when all different temporal components are mutually spatially uncorrelated at the input to the interaction region:  $\mathcal{E}_{i,j}^{\pm}(\mathbf{r})_{\text{in}} = 0$  for all  $i \neq j$ . Direct inspection of Eqs. (10) then reveals that these components remain uncorrelated throughout the interaction region no matter what the interaction geometry (the angle between the beams, full or partial intersection of the beams inside the crystal, and so on). Hence we are left with only  $N$  pairs of diagonalized equations for  $\mathcal{E}_{i,i}^{\pm}$  ( $1 \leq i \leq N$ ), with different indices coupled only through the common total intensity  $I_T$  in the denominators. In the one-dimensional case these equations are solvable trivially. For the two- or three-dimensional case one in general needs to resort to numerics, but even then the diagonalized equations are more transparent physically than the general system of Eqs. (10) for partially correlated fields.

Below we show that Eqs. (10) can always be cast in the diagonalized form discussed above at the cost of the following additional assumption. Assume that all input quadratic combinations for beams  $\mathcal{E}^{\pm}$  can be represented in the form

$$\mathcal{E}_{i,j}^{\pm}(\mathbf{r})_{\text{in}} = \alpha_{i,j} f^{\pm}(\mathbf{r}), \quad (15)$$

where  $\alpha_{i,j}$  are complex constants and  $f^{\pm}$  are some functions. In the reflexive coupling geometry they obey the relation  $\int d\mathbf{r} f^+(\mathbf{r}) = R \int d\mathbf{r} f^-(\mathbf{r})$ , where  $R$  is the

power ratio of the gain/loss beams. Condition (15) means that, statistically, all temporal components are beams with identical spatial envelopes (but possibly different fine structures) and at the input are characterized by coordinate-independent normalized mutual correlation functions  $h_{i,j}^{\pm}$  [Eq. (11)]. Note also that, because of the presence of the total intensity in the denominators of Eqs. (10), only the relative intensities of interacting features matter. This means that without loss of generality the functions  $f^{\pm}$  may be normalized in such a way that  $\int d\mathbf{r}f^+(\mathbf{r}) = R/(1+R)$  and  $\int d\mathbf{r}f^-(\mathbf{r}) = 1/(1+R)$ , and so diagonal elements of the matrix  $\hat{a}$  [Eq. (15)] are partial powers of temporal features obeying the relation  $\sum_{l=1}^N \alpha_{l,l} = 1$ .

Introduce new fields  $\tilde{e}_i^{\pm}$  such that

$$\tilde{e}_i^{\pm} = \sum_j T_{i,j} e_j^{\pm}, \quad (16)$$

where  $\hat{T}$  is a unitary matrix. Unitarity of  $\hat{T}$  means that the expression for the grating in new variables  $\tilde{e}^{\pm}$  retains the form of Eq. (3). Now require that the new fields be spatially uncorrelated at the input to the interaction region:  $\langle \tilde{e}_i^+ \tilde{e}_j^{+*} \rangle_{\text{in}} = \langle \tilde{e}_i^- \tilde{e}_j^{-*} \rangle_{\text{in}} = 0$  for  $i \neq j$ . This condition results in the equations  $\sum_l \langle e_l^{\pm*} e_l^{\pm} \rangle_{\text{in}} T_{j,l} = \langle |\tilde{e}_j^{\pm}|^2 \rangle_{\text{in}} T_{j,i}$ . Taking into account Eq. (15) and the fact that at the input all quadratic combinations of the fields  $\tilde{e}^+$  are characterized by the same coordinate dependence  $f^+(\mathbf{r})$  [and of  $\tilde{e}^-$  by the same dependence  $f^-(\mathbf{r})$ ], we may pull these coordinate dependencies out and get the following equation:

$$\hat{a} \mathbf{t}_j = \lambda_j \mathbf{t}_j, \quad 1 \leq j \leq N, \quad \mathbf{t}_j = (T_{j,1}, \dots, T_{j,N}), \quad (17)$$

where  $\langle |\tilde{e}_j^{\pm}|^2 \rangle_{\text{in}} = \lambda_j f^{\pm}(\mathbf{r})$ .

Equation (17) is the equation for eigenvectors and eigenvalues of matrix  $\hat{a}$ . Inasmuch as the matrices  $\hat{E}_{\text{in}}^{\pm}$ , and consequently  $\hat{a}$ , are Hermitian, such vectors exist and constitute an orthonormal set. These eigenvectors form the rows of the unitary matrix  $\hat{T}$ .

We showed by introducing the new set of fields  $\tilde{e}^{\pm}$  [Eq. (16)] that the system of equations for partially spatially correlated fields (10) can be cast in the diagonal form:

$$\frac{\partial}{\partial l_+} I_i^+(\mathbf{r}) = \frac{\Gamma}{I_T} I_i^+ I_i^-, \quad (18a)$$

$$\frac{\partial}{\partial l_-} I_i^-(\mathbf{r}) = -\frac{\Gamma}{I_T} I_i^+ I_i^-, \quad (18b)$$

$$I_T = \sum_{l=1}^N (I_l^+ + I_l^-), \quad (18c)$$

where  $1 \leq i \leq N$  and  $I_i^{\pm} = \langle \tilde{e}_i^{\pm*} \tilde{e}_i^{\pm} \rangle$ . The input boundary conditions for Eqs. (18) are

$$I_i^{\pm}(\text{in}) = \lambda_i f^{\pm}(\mathbf{r}), \quad (19)$$

where  $\lambda_i$  are the eigenvalues of Eq. (17) and the functions  $f^{\pm}$  are determined by relations (15). Once solutions of Eqs. (18) are known, quadratic combinations of the original fields can be found from the relations

$$\mathcal{E}_{i,j}^{\pm} = \sum_l I_l^{\pm}(\mathbf{r}) T_{l,i} T_{l,j}^*. \quad (20)$$

Note in conclusion that the above diagonalization procedure, though trivial in principle, for large  $N$  can be carried out only numerically. Analytical formulas are available for small values of  $N$ . Thus for  $N = 2$  one gets

$$\lambda_{1,2} = {}^{1/2}(\alpha_{1,1} + \alpha_{2,2} \pm s), \quad (21a)$$

$$T_{1,1} = -T_{2,2} = \left[ \frac{1}{2} + \frac{(\alpha_{1,1} - \alpha_{2,2})}{2s} \right]^{1/2}, \quad (21b)$$

$$T_{1,2} = T_{2,1} = \left[ \frac{1}{2} - \frac{(\alpha_{1,1} - \alpha_{2,2})}{2s} \right]^{1/2}, \quad (21c)$$

where  $s = [(\alpha_{1,1} - \alpha_{2,2})^2 + 4|\alpha_{1,2}|^2]^{1/2}$  (recall that  $\alpha_{2,1} = \alpha_{1,2}^*$ ).

#### 4. ASYMPTOTIC PROPERTIES OF SOLUTIONS

One can gain some insight into the behavior of solutions of Eqs. (10) by analyzing their asymptotic properties. We carry out this analysis below in the framework of a one-dimensional model. The one-dimensional transition in Eqs. (10), Eqs. (18), or both corresponds to the replacements  $\partial/\partial l_+ \rightarrow \cos(\theta/2)^{-1}(\partial/\partial x)$ ,  $f^+ \rightarrow Rf(y)/(1+R)$ , and  $f^- \rightarrow f(y)/(1+R)$ , where  $x$  and  $y$  are coordinates across and along the boundaries, respectively, of the nonlinear medium. Because of the presence of the total intensity in the denominators of the right-hand sides of Eqs. (10) and (18), all transverse coordinate dependencies (which are the same at the input) factor out. This means that the transverse coordinate distributions of the beams do not change because of the nonlinear interaction and that the normalized correlation functions remain constant over the beam cross sections.

The solutions of Eqs. (10) for large values of the nonlinearity ( $\Gamma L \rightarrow \infty$ ) are investigated best with the help of solutions of the diagonalized Eqs. (18) that have the form<sup>4</sup>

$$I_i^+(x, y) = f(y) \frac{\lambda_i R \exp(\gamma_i x)}{[1 + R \exp(\gamma_i x)]}, \quad (22a)$$

$$I_i^-(x, y) = f(y) \frac{\lambda_i}{[1 + R \exp(\gamma_i x)]}, \quad (22b)$$

where

$$\gamma_i = \frac{\Gamma}{\cos(\theta/2)} \frac{\lambda_i}{\sum_{l=1}^N \lambda_l}. \quad (23)$$

Consider first evolution of the loss beams  $I^-$ . For large values of  $\gamma_i x$  such that  $R \exp(\gamma_i x) \gg 1$  the loss beams become strongly depleted, and their intensities as functions of coordinates decrease exponentially with the negative growth rates  $-\gamma_i$ . Eventually a component with the smallest value of  $\lambda$  will become exponentially larger than the rest, dominating in inversion formulas (20) and selecting only one leading term out of the sums. The modulus of the normalized mutual correlation function  $h_{i,j}^-$  [Eq. (11)] between any two loss beams then tends to unity:  $|h_{i,j}^-| \rightarrow 1$ , indicating that all loss beams become com-

pletely spatially correlated at the output. Asymptotic coherence properties of the gain beams  $I^+$  are different. According to Eqs. (22)  $I_i \rightarrow f(y)\lambda_i$  for  $\gamma_i x \rightarrow \infty$ , so the relative intensities of the output gain beams remain the same as at the input. Inversion formulas (20) then show that the output normalized correlation functions (11) of the gain beams coincide with their input ones. One must note though that for intermediate values of nonlinearity such that  $R \exp(\gamma_i L) \leq 1$  the output gain beams may become almost completely correlated, provided that the gain/loss power ratio  $R$  is small enough. Indeed, as long as the gain beams remain weak, i.e.,  $R \exp(\gamma_i L) \leq 1$ , their spatial evolution is described by the growth rates  $\gamma_i$ , so a component with the largest value of  $\lambda$  will dominate in inversion formulas (20), resulting in all gain beams' being almost completely correlated at the output.

Consider now properties of solutions of Eqs. (10) in the situation when all the input features are nearly orthogonal and have nearly the same intensities. If all  $N$  temporal features are completely orthogonal and have the same intensities, solutions of Eqs. (10) have the form  $\mathcal{E}_{i,j}^\pm = \delta_{i,j} I^\pm$ , where  $I^\pm$  are given by Eqs. (22) and (23), with  $\lambda_i = 1/N$ ,  $1 \leq i \leq N$ :

$$I^+ = \frac{f(y)}{N} \frac{R \exp[\Gamma x/N \cos(\theta/2)]}{\{1 + R \exp[\Gamma x/N \cos(\theta/2)]\}}, \quad (24a)$$

$$I^- = \frac{f(y)}{N} \frac{1}{\{1 + R \exp[\Gamma x/N \cos(\theta/2)]\}}. \quad (24b)$$

Consider now an arbitrary set of temporal features in the vicinity of Eqs. (24) characterized by input normalized correlation functions  $h_{i,j}^{\text{in}}$  and partial intensities of temporal features  $\alpha_{i,i}$  ( $\sum \alpha_{i,i} = 1$ ) such that  $|h_{i,j}^{\text{in}}|^2 \ll 1/N$  and  $|\Delta\alpha_{i,i}| = |\alpha_{i,i} - 1/N| \ll 1/N$  for all  $i, j$ . Solution of Eqs. (10) in this limit gives the following expressions for the normalized correlation functions of the loss beams  $h_{i,j}^-$  and the relative deviations  $\epsilon_i(x) = \mathcal{E}_{i,i}^-(x, y)/I^-(x, y) - 1$  ( $\epsilon_i^{\text{in}} = N\Delta\alpha_{i,i}$ ) in the intensities of loss beam  $\mathcal{E}_{i,i}^-(x, y)$  from  $I^-$ :

$$h_{i,j}^{-,\text{out}} = F_1 h_{i,j}^{-,\text{in}} - F_2 h_{i,j}^{-,\text{in}} \frac{\epsilon_i^{\text{in}} + \epsilon_j^{\text{in}}}{2} - F_3 \sum_{l \neq i,j} h_{i,l}^{-,\text{in}} h_{l,j}^{-,\text{in}} + \dots, \quad (25a)$$

$$\epsilon_i^{\text{out}} = F_1 \epsilon_i^{\text{in}} - F_3 \left[ (\epsilon_i^{\text{in}})^2 + \sum_{l \neq i} |h_{i,l}^{-,\text{in}}|^2 \right] + \dots, \quad (25b)$$

where

$$F_1 = 1 - \frac{\tilde{\Gamma} R \exp(\tilde{\Gamma})}{1 + R \exp(\tilde{\Gamma})}, \quad (26a)$$

$$F_2 = \frac{\tilde{\Gamma} R \exp(\tilde{\Gamma})}{1 + R \exp(\tilde{\Gamma})} \left[ 1 + \frac{\tilde{\Gamma} R}{1 + R \exp(\tilde{\Gamma})} \right], \quad (26b)$$

$$F_3 = \frac{\tilde{\Gamma} R \exp(\tilde{\Gamma})}{1 + R \exp(\tilde{\Gamma})} \left[ 1 + \left( \frac{\tilde{\Gamma}}{2} \right) \frac{1 - R \exp(\tilde{\Gamma})}{1 + R \exp(\tilde{\Gamma})} \right], \quad (26c)$$

and  $\tilde{\Gamma} = \Gamma L/N \cos(\theta/2)$ .

Coherence properties at the gain port are described by the same relations [(25) and (26)] under the replacements  $\Gamma \rightarrow -\Gamma$  and  $R \rightarrow R^{-1}$ . Solutions (25) show the possibility of asymptotic orthogonalization of partially correlated

features in the reflexive coupling geometry at the loss port. Indeed, the leading terms in Eqs. (25) are proportional to the function  $F_1$ , so the requirement that  $F_1 = 0$  results in  $|\epsilon_i^{\text{out}}| < |\epsilon_i^{\text{in}}|$  and  $|h_{i,j}^{-,\text{out}}| < |h_{i,j}^{-,\text{in}}|$ . This requirement selects the value of  $\tilde{\Gamma} = \tilde{\Gamma}_{\text{orth}}$ , determined from the equation

$$(\tilde{\Gamma}_{\text{orth}} - 1) \exp(\tilde{\Gamma}_{\text{orth}}) = 1/R. \quad (27)$$

Equation (27) shows that the value of  $\tilde{\Gamma}_{\text{orth}}$  is not dependent on the exact spatiotemporal characteristics of the beam and ensures uniform convergence of any set of temporal features at the loss port to the completely orthogonal set [Eqs. (24)], provided that the input set of sufficiently close to being orthogonal. When there are only two spatiotemporal features, perfect orthogonalization is always possible for arbitrary input correlations.<sup>4</sup> Note also [Eq. (26)] the replacements  $\Gamma \rightarrow -\Gamma$  and  $R \rightarrow R^{-1}$ , and the equation  $F(1) = 0$  has no solution.

## 5. NUMERICAL RESULTS

Properties of solutions of Eqs. (10) and (18) for arbitrary values of nonlinearity and boundary conditions are illustrated by several numerical examples below. Figures 2–4 represent typical solutions of Eqs. (10) for  $N = 2$  in the full two-dimensional and Figs. 5 and 6 in the one-dimensional cases, respectively. The boundary conditions are chosen of the form

$$\mathcal{E}_{1,1}^{+,\text{in}} = \frac{q_1 R}{(1 + R)} f(y), \quad \mathcal{E}_{2,2}^{+,\text{in}} = \frac{q_2 R}{(1 + R)} f(y), \quad (28a)$$

$$\mathcal{E}_{1,2}^{+,\text{in}} = H_{1,2}^{\text{in}} \sqrt{q_1 q_2} \frac{R}{(1 + R)} f(y), \quad (28b)$$

$$\mathcal{E}_{1,1}^{-,\text{in}} = \frac{q_1}{(1 + R)} f(x), \quad \mathcal{E}_{2,2}^{-,\text{in}} = \frac{q_2}{(1 + R)} f(x), \quad (28c)$$

$$\mathcal{E}_{1,2}^{-,\text{in}} = H_{1,2}^{\text{in}} \sqrt{q_1 q_2} \frac{1}{(1 + R)} f(x), \quad (28d)$$

where  $f(\xi) = 1/\sqrt{\pi} \exp(-\xi^2)$  and  $q_i = \alpha_{i,i}$  ( $i = 1, 2$ ) are relative intensities of temporal features 1 and 2 ( $q_1 + q_2 = 1$ ),  $H$  is their initial degree of overlap ( $0 \leq |H| \leq 1$ ), and  $R$  is the gain/loss beams' power ratio. In the full two-dimensional case (Figs. 2–4)  $\delta \gg 1$ , so the beam overlap region lies inside the nonlinear medium; in the one-dimensional limit (Figs. 5 and 6)  $\delta = 0.3$ , and the overlap region is mostly outside. For both cases  $q_1 = 0.6$ ,  $q_2 = 0.4$ ,  $H_{1,2}^{\text{in}} = 0.7$ , and  $R = 0.5$ .

Figure 2(a) shows powers  $P_{1,1}^{+,\text{out}}$  and  $P_{2,2}^{+,\text{out}}$  of temporal features 1 and 2 at the gain port and their integrated correlation function  $P_{1,2}^{+,\text{out}}$  (solid curves) versus nonlinearity and also the modulus of the overlap  $H_{1,2}^{+,\text{out}}$  between temporal features 1 and 2 at the gain port [ $P_{i,j}$  and  $H_{i,j}$  are determined by relations (12)]. Figure 2(b) shows the same for the loss port.

Figure 3(a) shows output intensity distributions  $\mathcal{E}_{1,1}^{+,\text{out}}$  and  $\mathcal{E}_{2,2}^{+,\text{out}}$  of temporal features 1 and 2 at the gain port and the correlation function  $\mathcal{E}_{1,2}^{+,\text{out}}$  for the case when the beam overlap region lies entirely inside the medium and for the value of nonlinearity  $3\Gamma d/\sin(\theta) = 7.5$ . Figure 3(b) shows the same for the loss port.

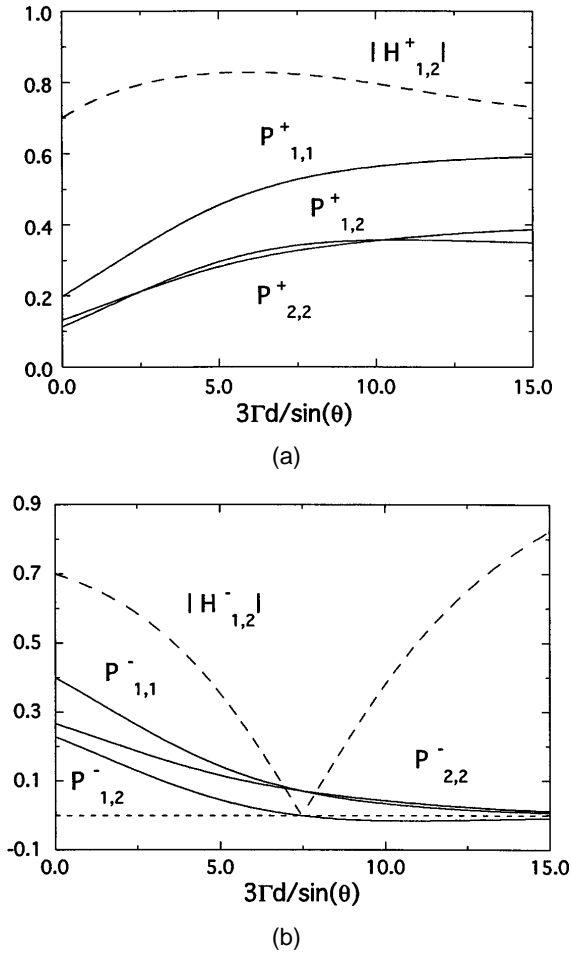


Fig. 2. Integral output characteristics of temporal features 1 and 2 at (a) the gain and (b) the loss ports as functions of nonlinearity for  $\delta \gg 1$ . The solid curves correspond to  $P_{1,1}^{\text{out}}$ ,  $P_{2,2}^{\text{out}}$ , and  $P_{1,2}^{\text{out}}$ ; the dashed curve, to  $|H_{1,2}^{\text{out}}|$ .

Figure 4 shows normalized output correlation functions [Eq. (11)]  $h_{1,2}^{+, \text{out}}$  and  $h_{1,2}^{-, \text{out}}$  for temporal features 1 and 2 at gain and loss ports, respectively, for the conditions of Fig. 3.

Figures 5(a) and 5(b) are identical to Figs. 2(a) and 2(b) and show output powers and integrated correlation functions at the gain point [Figs. 2(a) and 5(a)] and the loss port [Figs. 2(b) and 5(b)] but in the case when the beam overlap region lies mostly outside the medium ( $\delta = 0.3$ ). For the one-dimensional limit we do not present spatial distributions of intensities (corresponding to those given in Fig. 3). The normalized output correlation functions at the gain and the loss ports, given by Fig. 6 (analogous to Fig. 4), are more interesting.

Figures 2 and 5 demonstrate that the correlation functions and overlaps at the gain and the loss ports evolve quite differently at functions of nonlinearity. The overlap between the temporal features at the gain port remains more or less the same, whereas that at the loss port passes through zero. This behavior is easy to explain. Indeed, it follows from Eqs. (20) and (21) that  $E_{1,2}(\mathbf{r}) \propto I_1(\mathbf{r}) - I_2(\mathbf{r})$  and hence  $P_{1,2} \propto P_1 - P_2$ , where  $P_{1,(2)}$  are the powers of mutually orthogonal loss beams. Suppose that  $\lambda_2 \leq \lambda_1$ , i.e., that  $P_2^{\text{in}} \leq P_1^{\text{in}}$ ; then the loss beam corresponding to a larger value of  $\lambda$  loses energy faster, and for large nonlinearities its output power

becomes less than that of the other beam. This is particularly easy to see from formulas (22) and (23), which describe evolution of the system in the framework of the one-dimensional model. For large nonlinearities the input and the output differences  $P_1 - P_2$  have different signs, so for some value of nonlinearity the output differ-

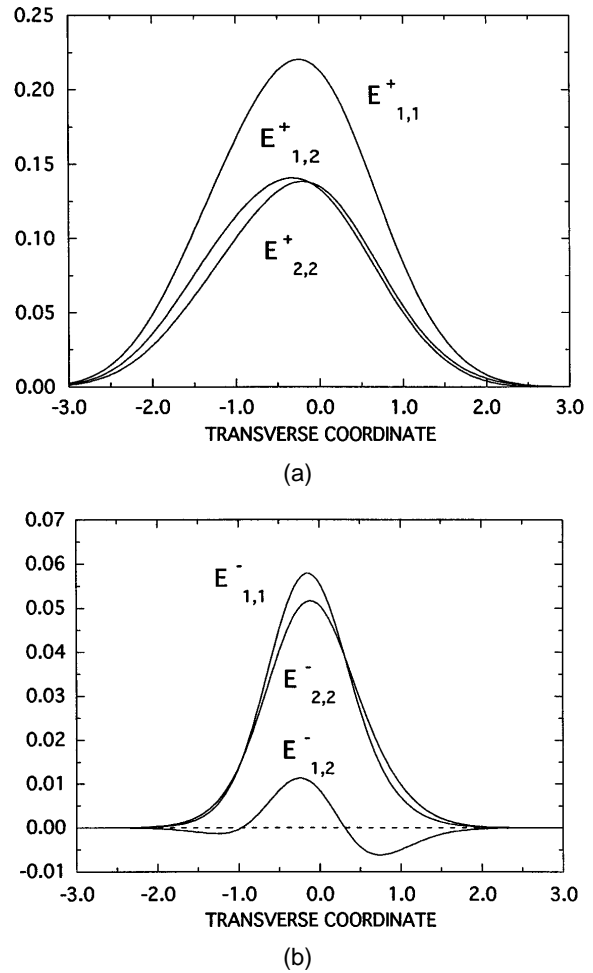


Fig. 3. Output intensity distributions and correlation functions of temporal features 1 and 2: (a) the gain port ( $E_{1,1}^{+, \text{out}}$ ,  $E_{2,2}^{+, \text{out}}$ ,  $E_{1,2}^{+, \text{out}}$ ) and (b) the loss port ( $E_{1,1}^{-, \text{out}}$ ,  $E_{2,2}^{-, \text{out}}$ ,  $E_{1,2}^{-, \text{out}}$ ) for  $\delta \gg 1$  and  $3\Gamma d/\sin(\theta) = 7.5$ .

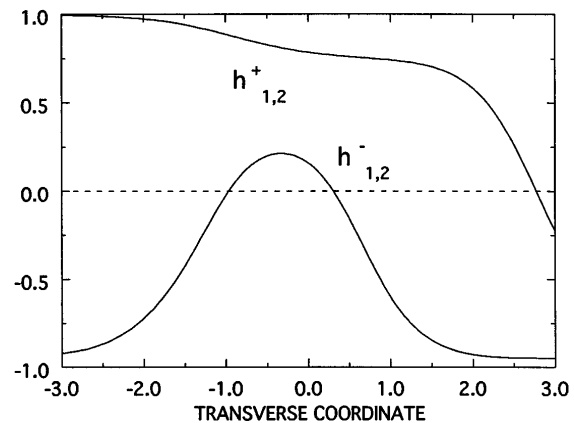


Fig. 4. Output normalized correlation functions  $h_{1,2}^{+, \text{out}}$  and  $h_{1,2}^{-, \text{out}}$  for  $\delta \gg 1$  and  $3\Gamma d/\sin(\theta) = 7.5$ .

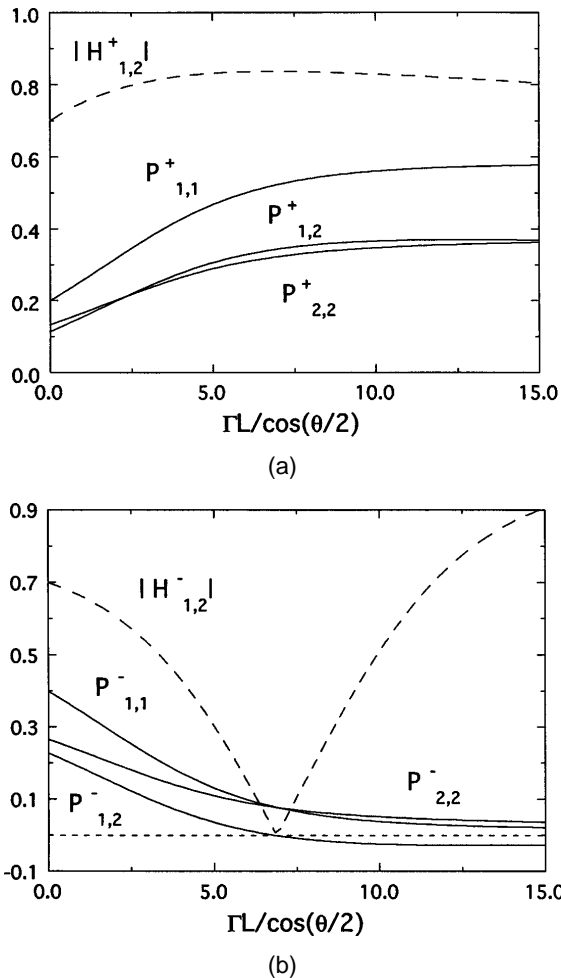


Fig. 5. Integral output characteristics of temporal features 1 and 2 at (a) the gain and (b) the loss ports as functions of nonlinearity for  $\delta = 0.3$ . The solid curves correspond to  $P_{1,1}^{\text{out}}$ ,  $P_{2,2}^{\text{out}}$ , and  $P_{1,2}^{\text{out}}$ ; the dashed curve, to  $|H_{1,2}^{\text{out}}|$ .

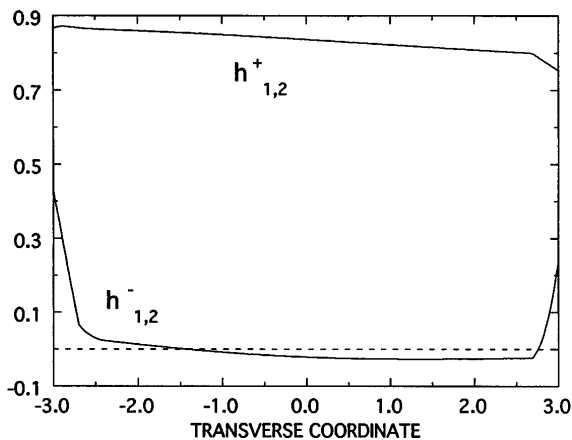


Fig. 6. Output normalized correlation functions  $h_{1,2}^{+,out}$  and  $h_{1,2}^{-,out}$  for  $\delta = 0.3$  and  $\Gamma L/\cos(\theta/2) = 7.4$ .

ence  $P_1 - P_2$  is exactly equal to zero. This corresponds to zero overlap between beams  $e_1^-$  and  $e_2^-$  at the output.

Figures 3 and 4 show that in the case when the beams overlap fully inside the nonlinear medium their initially Gaussian distributions become distorted at the output. This distortion corresponds to the intensity distributions

of the gain and loss beams shifting outward (loss beams in the minus  $x$  and gain beams in the minus  $y$  directions) and repelling each other.<sup>10</sup> At the very moderate values of nonlinearity corresponding to Figs. 3 and 4 the amount of this shift is small, but the effect becomes very pronounced for higher values of nonlinearity. The normalized mutual correlation functions at both ports become strongly inhomogeneous over the beams' cross sections. At the wings of the loss beams,  $|h_{1,2}^-|_{\text{out}} \rightarrow 1$  (Fig. 4). This feature is in agreement with our previous arguments about weak loss beams' becoming completely correlated. The same happens with the gain beams (Fig. 4, curve  $h_{1,2}^+$ ) but only at one edge (positive  $y$ ) where small-intensity gain beams cross large-intensity loss beams. On the opposite side (negative  $y$ ) the gain beams pass through the region of strongly depleted loss beams, and the level of nonlinearity is not enough to make them completely correlated.

Figures 5 and 6 correspond to the case when the beam overlap region lies mostly outside the nonlinear medium. This is the one-dimensional limit when partial derivatives in Eqs. (10) and (18) may be replaced by one common derivative in the direction perpendicular to the nonlinear medium boundaries. Figure 6 shows that the normalized correlation functions remain constant over the beams' cross sections except in the wings, meaning that the transverse coordinate distributions of the beams do not change because of the nonlinear interaction. Despite the different behavior of local correlation functions in Figs. 4 and 6 the integral characteristics of the interaction (Figs. 2 and 5) for the two limits are remarkably similar, showing that the one-dimensional model may be a good approximation even for a two-dimensional interaction geometry.

To balance this last statement we should note, though, that stretching the similarity between the two-dimensional case and the one-dimensional limit too far may sometimes be dangerous. In the case of the beam overlap region's lying inside the nonlinear medium the interaction changes both the spatial profiles of the beams and their local correlation functions (Figs. 3 and 4). On the contrary, in the one-dimensional limit all transverse dependencies factor out. Hence one may expect differences when these distortions are relatively large (large nonlinearities) and when the input correlation functions are coordinate dependent. To illustrate this point, let us consider solutions of Eqs. (10) with boundary conditions that are similar to those of Eqs. (28), except that the input mutual correlation functions are taken to be coordinate dependent:

$$\begin{aligned} \mathcal{E}_{1,2}^{+,in} &= \text{sign}(y)\sqrt{q_1q_2} \frac{R}{(1+R)} f(y), \\ \mathcal{E}_{1,2}^{-,in} &= \text{sign}(x)\sqrt{q_1q_2} \frac{1}{(1+R)} f(x) \end{aligned} \quad (29)$$

[notation is as in Eqs. (28)]. Boundary conditions (29) correspond to beams that are orthogonal at the input (the overlap integral is equal to zero) but nevertheless correlated. Figure 7 shows the moduli of the output overlaps  $H_{1,2}^{\text{out}}$  of temporal features 1 and 2 at the gain port (curve  $H_{1,2}^+$ ) and the loss port (curve  $H_{1,2}^-$ ) as functions of nonlinearity in the case when the beams fully cross inside the nonlinear medium. Initially orthogonal beams

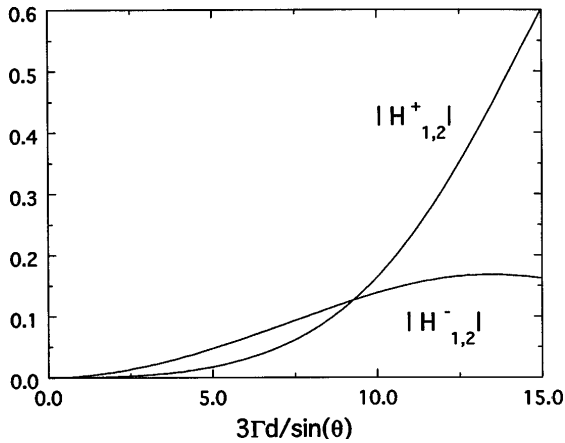


Fig. 7. Moduli of the output overlaps at the gain and the loss ports in the case of orthogonal but correlated input beams. The beam overlap region lies inside the nonlinear medium,  $q_1 = 0.6$ ,  $q_2 = 0.4$ ,  $H = 1$ , and  $R = 0.1$ .

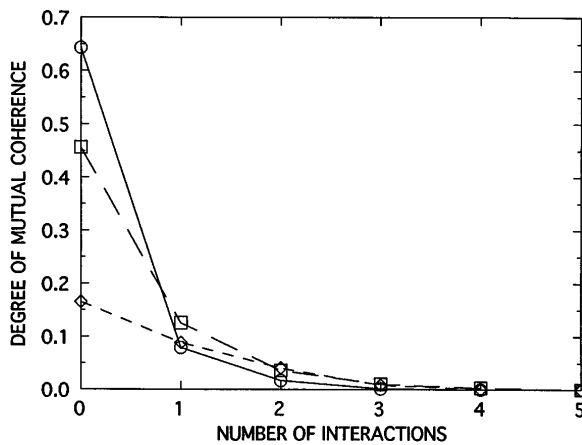


Fig. 8. Orthogonalization of five temporal features: average output degree of mutual coherence as the function of the number of interactions ( $R = 0.5$ ,  $\Gamma L = 7.3$ ).

become strongly spatially overlapped at the output. The same output overlaps in the one-dimensional limit would remain zero.

One of the interesting features of the reflexive coupling geometry is its ability to correlate or orthogonalize partially overlapping temporal features. In general this requires processing the beam in several reflexive coupling geometries (several photorefractive crystals). Thus, to orthogonalize the features, the beam emerging at the loss port of the first reflexive coupling geometry (first crystal) should be sent to a second crystal. The beam emerging at the loss port of the second reflexive coupling geometry is sent to a third crystal, and so on. The nonlinearity and the gain/loss beams power ratio in each crystal are adjustable parameters chosen to ensure convergence of this procedure to a set of completely orthogonal temporal features. Figure 8 shows three examples of orthogonalization of five temporal features ( $N = 5$ ) by use of a succession of reflexive coupling geometries as discussed above. We obtained the curves by solving Eqs. (10) numerically in the one-dimensional limit. Initial intensities and complex degrees of mutual correlation were generated randomly for each of the plots. The abscissa shows the number of interactions (crystals) with crystal

number zero corresponding to initial conditions. The ordinate is the average degree of output correlation at the loss port  $\eta = [1/N(N-1)]\sum_{i \neq j} |h_{i,j}^{-,out}|^2$ . The value of  $\Gamma L$  for all crystals was kept the same and set equal to  $\bar{\Gamma}_{orth}N \approx 7.3$  [see Eq. (27)] for the chosen gain/loss power ratio  $R = 0.5$ . Use of different values of  $\Gamma L$  and  $R$  in different crystals based on detailed information about initial intensities and the mutual degrees of overlap in each particular case would permit achievement of more rapid convergence to the final orthogonal state. On the other hand, Fig. 8 shows that using the value  $\bar{\Gamma}_{orth}$  may be a good choice when there exists no *a priori* knowledge about the pictorial information carried by the beam.

## 6. SUMMARY

Photorefractive reflexive coupling is a two-beam mixing process of an information-bearing beam carrying several spatiotemporal features with a copy of itself in a photorefractive medium. It allows one to manipulate information carried by the beam by changing both the relative intensities and the degrees of mutual coherence of the features. We formulated general equations describing the photorefractive coupling geometry in terms of mutual transverse correlation functions of the features and discussed the parameters that affect the interaction geometry in the case of full or partial overlap of the interacting beams inside the nonlinear medium. We showed that general nonlinear equations for partially spatially correlated features can be diagonalized under certain assumptions. This implies the existence of a unitary transformation from the initial set of input features to their combinations that remain spatially uncorrelated throughout the interaction region. We analyzed asymptotic coherence properties of the reflexive coupling geometry in several limiting cases. Coherence properties for arbitrary values of the nonlinearity and boundary conditions were illustrated by numerical solutions corresponding to both the full two-dimensional case and the limit leading to a one-dimensional description of the geometry.

## ACKNOWLEDGMENTS

The research at the Joint Institute for Laboratory Astrophysics was supported by National Science Foundation (NSF) grant PHY90-12244 and the Optoelectronic Computing Systems Center, an NSF Engineering Research Center. That at Risø was supported by Danish Natural Science Research Council grant 9401024.

## REFERENCES

1. N. V. Bogodaev, L. I. Ivleva, A. S. Korshunov, N. M. Polozkov, and V. V. Shkunov, "Increase of light-beam coherence of two-wave mixing in photorefractive crystals," *J. Opt. Soc. Am. B* **10**, 2287–2289 (1993).
2. H. Kong, C. Wu, and M. Cronin-Golomb, "Photorefractive two-beam coupling with reduced spatial coherence," *Opt. Lett.* **16**, 1183–1185 (1991).
3. M. Cronin-Golomb, H. Kong, and W. Królikowski, "Photorefractive two-beam coupling with light of partial spatiotemporal coherence," *J. Opt. Soc. Am. B* **9**, 1698–1703 (1992).
4. D. Z. Anderson, M. Saffman, and A. Hermans, "Manipulating the information carried by an optical beam with reflexive photorefractive beam coupling," *J. Opt. Soc. Am. B* **12**, 117–123 (1995).

5. M. Saffman, C. Benkert, and D. Z. Anderson, "Self-organizing photorefractive frequency demultiplexer," *Opt. Lett.* **16**, 1993–1995 (1991).
6. D. Z. Anderson, C. Benkert, V. Hebler, J.-S. Jang, D. Montgomery, and M. Saffman, "Optical implementation of a self-organizing feature extractor," in *Advances in Neural-Information Processing Systems IV*, J. E. Moody, S. J. Hanson, and R. P. Lippmann, eds. (Morgan Kaufmann, San Mateo, Calif., 1992), pp. 821–828.
7. D. Chomsky, S. Sternklar, A. Zigler, and S. Jackel, "Laser frequency bandwidth narrowing by photorefractive two-beam coupling," *Opt. Lett.* **17**, 481–483 (1992).
8. S. M. Rytov, Yu. A. Kravtsov, and V. I. Tatarskii, *Principles of Statistical Radiophysics* (Springer-Verlag, Berlin, 1989), Vol. 4.
9. A. A. Zozulya, V. P. Silin, and V. T. Tikhonchuk, "The theory of phase conjugation during stimulated scattering in a self-intersecting light beam," *Zh. Eksp. Teor. Fiz.* **92**, 788–800 (1987) [*Sov. Phys. JETP* **65**, 443–449 (1987)].
10. A. A. Esayan, A. A. Zozulya, and V. T. Tikhonchuk, "Energy exchange under conditions of a two-beam interaction in a photorefractive medium," *Kvantovaya Elektron. (Moscow)* **18**, 1340–1346 (1991) [*Sov. J. Quantum Electron.* **21**, 1225–1230 (1991)].